Asian Journal of Chemistry; Vol. 37, No. 12 (2025), 3158-3166
ASIAN JOURNAL OF CHEMISTRY
https://doi.org/10.14233/ajchem.2025.34793

Design, Synthesis and Evaluation of Novel Quinoline-Thiazolidinone-Isonicotinamide Hybrids as Potent InhA Inhibitors for Antitubercular Therapy

SATENDRA KUMAR[1,2] and NIRANJAN KAUSHIK[1,*]

[1]Department of Pharmacy, School of Medical & Allied Sciences, Galgotias University, Gautam Budh Nagar-201310, India
[2]SRM Modinagar College of Pharmacy, Faculty of Medicine & Health Sciences, SRM Institute of Science and Technology, NCR Campus, Delhi-Meerut Road, Modinagar, Ghaziabad-201204, India

*Corresponding author: E-mail: niranjankaushik79@gmail.com

Received: 27 July 2025 *Accepted*: 15 November 2025 *Published online*: 30 November 2025 AJC-22207

A series of quinoline–thiazolidinone–isonicotinamide hybrids (**SK-1** to **SK-12**) was design, synthesized and characterized for their potential as antitubercular agent. The hybrid compounds were synthesized through a cyclization reaction using thioglycolic acid, affording yields of 63-76% with high stereoselectivity and their structure were confirmed by IR, ^{1}H, ^{13}C NMR, MS and elemental analysis. Molecular docking studies against *M. tuberculosis* Enoyl-ACP Reductase (InhA) revealed high binding affinities (-9.3 to -7.5 kcal/mol) significantly better than that of isoniazid (-7.5 kcal/mol) primarily mediated by hydrogen bonds with active-site residues such as ASP54, PHE149 and TYR158. ADMET prediction indicated drug-likeness, effective gastrointestinal absorption, low blood–brain barrier permeability and reduced risk of mutagenicity and carcinogenicity. *In vitro* antitubercular assay was performed by Microplate Alamar Blue Assay (MABA) and Low Oxygen Recovery Assay (LORA) methods, results showed that derivatives **SK-3**, **SK-5** and **SK-6** exhibited significant antitubercular activity as compared to isoniazid.

Keywords: Hybrid molecules, Quinoline, Thiazolidinone, Isonicotinamide, InhA inhibition, Antitubercular agents, Molecular docking.

INTRODUCTION

Tuberculosis causes *Mycobacterium tuberculosis* remains a major global public health challenge. It is responsible for over 10 million new cases and 1.5 million deaths annually. The situation is exacerbated by the increasing prevalence of multi-drug-resistant (MDR) and extensively drug-resistant (XDR) strains [1-3]. The advent of antimicrobial resistance (AMR) has compromised the efficacy of first-line therapies like isoniazid, rifampicin and pyrazinamide. This underscores the urgent need for novel multi-targeting agents that can overcome resistance mechanisms while exhibiting low toxicity and favourable pharmacokinetic profiles [4]. Quinoline (a) derivatives have been central to antimicrobial drug discovery since the early days, as represented by bedaquiline (b), a diarylquinoline (c) used in MDR-TB that targets mycobacterial ATP synthase, and by early antimalarials such as chloroquine and mefloquine (d), which act on the heme detoxification pathway in the *Plasmodium parasite* [5-7].

Recent reviews highlight the versatility of the quinoline scaffold, where structural modifications can enhance anti-tubercular activity through mechanisms such as DNA gyrase inhibition, efflux pump modulation and synergistic effects in drug combinations [8]. Thiazolidinones represent another privileged scaffold, demonstrating broad-spectrum antimicrobial activity by interfering with bacterial cell wall integrity, inhibiting enzymes like MurB in peptidoglycan biosynthesis and exerting antioxidant effects that mitigate oxidative stress in host cells [9]. Isoniazid, a first-line TB prodrug, exerts its effect by inhibiting mycolic acid biosynthesis after activation by the bacterial catalase-peroxidase (KatG). However, its efficacy is severely limited by katG mutations in resistant strains.

Hybridization approaches by merging these moieties have become popular in order to obtain synergistic effects, better bioavailability and lower resistance development [10]. For example, quinoline-isoniazid conjugates have enhanced anti-mycobacterial potency (MIC values as low as 0.95 μM against clinical isolates), quinoline-thiazolidinone hybrids exhibit strong inhibition of *M. tuberculosis* H37Rv strain through dual action on DNA and cell wall components [11,12]. Similarly, isoniazid-thiazolidinone hybrids have shown promising antifungal and antibacterial activities, underscoring the potential of such hybrid

frameworks [13-16]. Despite these advancements, no prior studies have reported on the specific triad comprising a 2-hydroxy-quinoline-3-yl moiety linked to a 4-oxothiazolidine ring and an isonicotinamide group, particularly with strategic modifications at the 7-position (*e.g.* alkyl, haloalkyl, aryl) to optimize lipophilicity and target binding [17]. This gap in the literature presents an opportunity to develop novel hybrids that capitalize on the antimycobacterial heritage of quinolines, membrane-disrupting properties of thiazolidinones and targeted action of isoniazid, aiming to effective multi-targeting agents against MDR-TB [18]. In this study, we report the synthesis of 12 novel quinoline-thiazolidinone-isonicotinamide hybrids (**SK-1** to **SK-12**). The compounds were fully characterized by spectroscopic techniques and *in silico* analysis, including molecular docking against TB targets, QSAR modeling, ADMET profiling using SwissADME and pkCSM and toxicity prediction with ProTox-3.0. This research is directed towards identifying lead compounds with high efficacy, low toxicity and favourable drug-like properties for subsequent preclinical development.

EXPERIMENTAL

All chemicals and reagents (analytical grade) were purchased from Sigma-Aldrich and used without further purification. Melting points were determined using a Fisher-Johns apparatus and are uncorrected. The thin-layer chromatography was performed on coated silica gel 60 F_{254} plates to monitor the progress of the reaction. A 630 FTIR spectrometer model Agilent MicroLab was used to measure the infrared (IR) spectra using KBr in the range of 4000-400 cm^{-1}. ^1H and ^{13}C NMR spectra were recorded on a Bruker AV-300 spectrometer (300 MHz for ^1H, 75 MHz for ^{13}C using $CDCl_3$ or DMSO-d_6 as solvents.

General procedure for synthesis of substituted 2-chloroquinoline-3-carbaldehyde (1a-1l): DMF was added drop by drop to the solution of substituted N-phenylacetamide, which was cooled to 0 ºC in a flask with a drying tube while stirring. Then, 0.350 mol of phosphorus oxychloride in 32.2 mL was added. After 5 min, the solution was kept under reflux for 16 h. The reaction mixture was then mixed with 300 mL of cold water and agitated for 30 min at 0-10 ºC, which results in the formation of substituted-2-chloroquinoline-3-carbaldehyde (**1a-l**) as a yellow precipitate (**Scheme-I**). It was filtered, washed with distilled water and then recrystallized from ethyl acetate show as.

Synthesis of substituted-2-hydroxyquinoline-3-carbaldehyde (2a-2l): In the subsequent step, a mixture of substituted 2-chloroquinoline-3-carbaldehyde (1.9 g, 0.01 mol) and NaOH (35 mL, 4 M) and 35 mL ethanol was heated under reflux for 1 h. After completion, the reaction mixture was allowed to cool to room temperature and then poured onto crushed ice, resulting in the formation of a yellow solid of substituted 2-hydroxyquinoline-3-carbaldehyde (**2a-2l**) (**Scheme-I**). The precipitated solid was filtered, washed thoroughly with water and dried. The crude product was recrystallized from aqueous acetic acid to afford the purified compound.

Synthesis of Schiff base substituted N-((2-hydroxyquinolin-3-yl)methylene)isonicotinohydrazide (intermediate) (3a-3l): A mixture of substituted 2-hydroxyquinoline-3-carbaldehyde (0.18 mol) (**2a-2l**) in DMSO (20 mL), isoniazid (0.18 mol) in ethanol (20 mL) and glacial acetic acid (0.30 mL) was refluxed for 7-8 h. The reaction mixture was then allowed to cool to room temperature, leading to the formation of a solid precipitate. The precipitate was filtered, washed with water and recrystallized from methanol to afford the Schiff base intermediate N-((2-hydroxyquinolin-3-yl)methylene)isonicotinohydrazide.

Cyclization of N-((2-hydroxyquinolin-3-yl)-4-oxothiazolidin-3-yl)isonicotinamide with thioglycolic acid: A mixture of substituted N-((2-hydroxyquinolin-3-yl)methylene)-isonicotinohydrazide derivatives (**3a-3l**) (0.2 mol) in DMSO (20 mL) with thioglycolic acid (0.2 mol), which was heated under reflux for 7-9 h. The reaction mixture was then cooled, filtered, rinsed with water and dried. The compounds were purified by column chromatography using ethyl acetate/hexane (1:2 to 2:3), affording the final products as pure crystalline solids (**Scheme-I**).

***N*-(2-(2-Hydroxyquinolin-3-yl)-4-oxothiazolidin-3-yl)-isonicotinamide (SK-1):** Pure white to off-white crystalline solid (yield: 65%; m.p.: 191-193 ºC; R_f = 0.65); IR (KBr, ν_{max}, cm^{-1}): 3401 (NH), 3207 (OH), 2916 (CH), 1703 (C=O), 1541 (C=C), 1451 (C–C), 1302 (C–N), 1164 (CS); ^1H NMR (400 MHz, DMSO-d_6, δ ppm): 9.76 (s, 1H, OH), 7.22–8.48 (m, 8H, Ar–H), 3.85 (s, 2H, CH_2), 1.19 (s, 1H, NH); ^{13}C NMR (100 MHz, DMSO-d_6, δ ppm): 175 (1C, CS), 166 (2C, C=O), 123–150 (14C, Ar–C), 35 (1C, C–C). m.f.: $C_{18}H_{14}N_4O_3S$. MS (*m/z*): 366 (M^+).

***N*-(4-Oxo-2-(2,5,7-trihydroxyquinolin-3-yl)thiazolidin-3-yl)isonicotinamide (SK-2):** White solid; yield: 70%; m.p.: 201-203 ºC; R_f value 0.5; IR (KBr, ν_{max}, cm^{-1}): 3401 (NH), 3207 (OH), 3091 (CH), 1703 (C=O), 1541 (C=C), 1451 (C–C), 1302 (CN) and 1164 (CS); ^1H NMR (400 MHz, DMSO-d_6, δ ppm): 9.76 (s, 1H, OH), 7.22-8.48 (m, 8H, Ar–CH), 3.85 (s, 2H, CH_2) and 1.19 (s, 1H, NH); ^{13}C NMR (100 MHz, DMSO-d_6, δ ppm): 176 (1C, CS), 166 (2C, C=O), 123-150 (14C, Ar–CH) and 35 (1C, C–C). m.f.: $C_{18}H_{14}N_4O_5S$; MS *m/z*: 398 (M^+).

***N*-(2-(2-Hydroxy-7-methylquinolin-3-yl)-4-oxothiazolidin-3-yl)isonicotinamide (SK-3)**: Yellowish solid; yield: 68%; m.p.: 179-181 ºC, R_f value 0.62; IR (KBr, ν_{max}, cm^{-1}): 3103 (OH), 2991 (CH), 1654 (C=O), 1507 (C=C), 1484 (C–C), 1162 (CS); ^1H NMR (400 MHz, DMSO-d_6, δ ppm): 9.76 (s, 1H, OH), 7.69-7.74 (d, 8H, ArH), 3.37 (s, 1H, NH), 3.62-3.88 (s, 2H, CH_2), 1.16 (s, 3H, CH); ^{13}C NMR (100 MHz, DMSO-d_6, δ ppm): 163-165 (2C, C=O), 122-148 (14C, Ar–CH), 37 (1C, CS), 22, (1C, CC), m.f.: $C_{19}H_{16}N_4O_3S$; MS *m/z*: 380 (M^+).

N-(2-(7-Ethyl-2-hydroxyquinolin-3-yl)-4-oxothiazolidin-3-yl)isonicotinamide (SK-4): Light brown solid (yield: 63%; m.p.: 162 -164 ºC; R_f value: 0.63); IR (KBr, ν_{max}, cm^{-1}): 3401 (NH), 3103 (OH), 2931 (CH), 1647 (C=O), 1589 (C=C) and 1166 (CS); ^1H NMR (400 MHz, $CDCl_3$, δ ppm): 9.86 (s, 1H, OH), 7.31- 7.48 (m, 8H, Ar–CH), 3.95-3.99 (s, 2H, CH_2), 2.88 (s, 2H, CH_2), 1.25-1.42 (s, 3H, CH), 0.88-1.26 (s, 3H, CH_3), 7.26 (s, $CDCl_3$); ^{13}C NMR (100 MHz, DMSO-d_6, δ ppm): 163-166 (2C, C=O), 125-143 (14C, ArC), 59 (1C, C–C) and 37 (1C, CS). m.f.: $C_{20}H_{18}N_4O_3S$. MS (*m/z*): 394 (M^+).

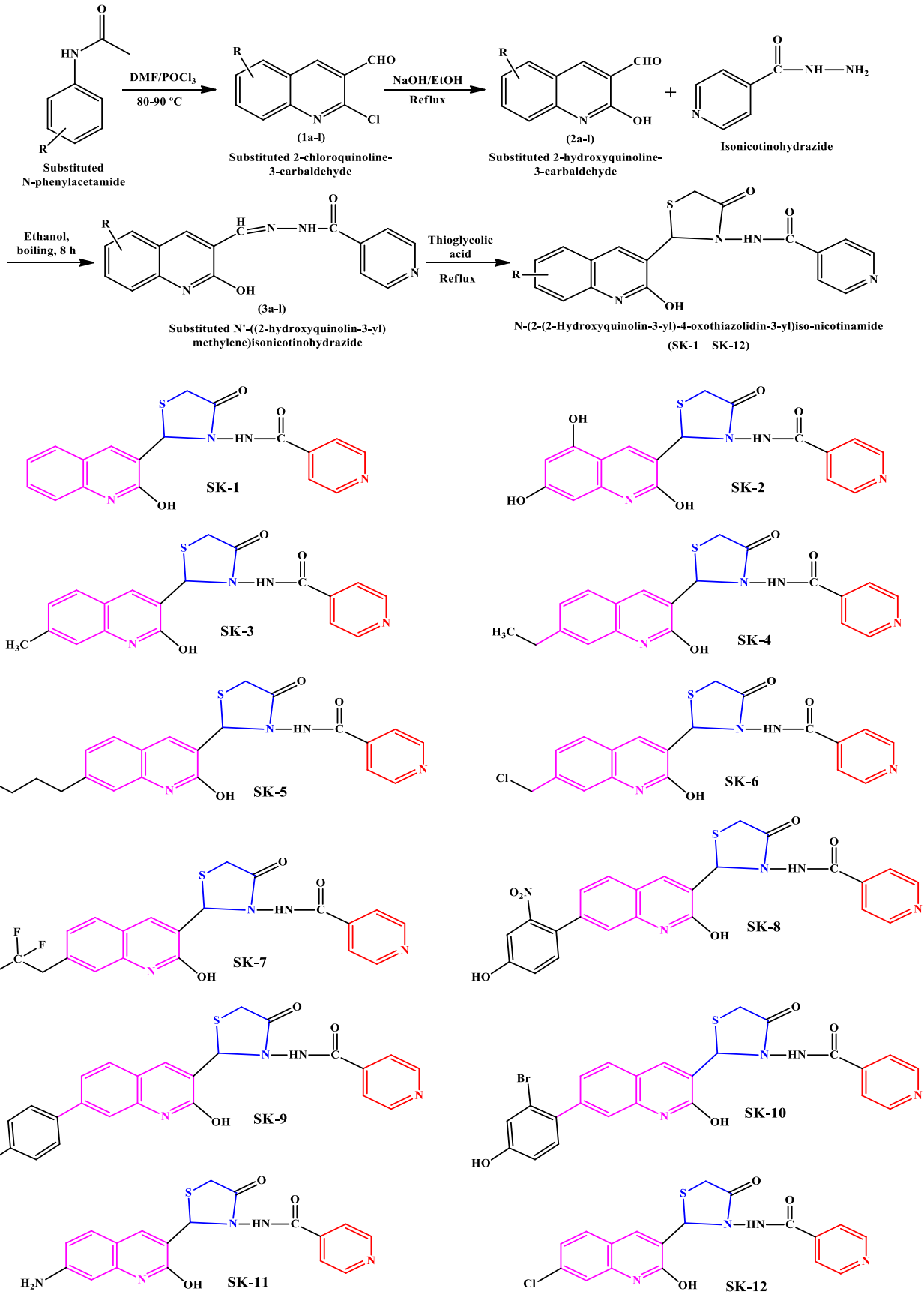

Scheme-I: Synthesis of quinoline-isonicotinohydrazide derivatives

***N*-(2-(7-Butyl-2-hydroxyquinolin-3-yl)-4-oxothiazolidin-3-yl)isonicotinamide (SK-5):** Pale yellow solid (yield: 72%; m.p.: 167-169 ºC; R_f value: 0.72). IR (KBr, ν_{max}, cm^{-1}): 3401 (NH), 3179 (OH), 2916 (CH), 1647 (C=O), 1517 (C=C) and 1194 (CS); ^{1}HNMR (400 MHz, $CDCl_3$, δ ppm): 10.16 (s, 1H, OH), 8.03-8.09 (m, 8H, Ar–CH), 3.07-4.52 (s, 4H, CH_2), 1.87–2.35 (s, 5H, CH_3); ^{13}C NMR (100 MHz, $CDCl_3$, δ ppm): 166.0 (2C, CO), 123.0-148.0 (14C, Ar–CH), 55.0 (2C, C–C) and 35.0 (1C, CS). m.f.: $C_{22}H_{22}N_4O_3S$. MS (*m/z*): 422 (M^+).

***N*-(2-(2-Hydroxy-3-(3-(isonicotinamido)-4-oxothiazolidin-2-yl)quinolin-7-yl)methyl hypochlorite (SK-6):** Light cream solid (yield: 64%; m.p.: 188-190 ºC; R_f value: 0.62); IR (KBr, ν_{max}, cm^{-1}): 3384 (NH), 3093 (OH), 2916 (CH), 1691 (C=N), 1677 (CO), 1591 (C=C), 1490 (C–C), 1175 (C–S), 972 (CH) and 760 (Cl); ^{1}H NMR (400 MHz, $CDCl_3$, δ ppm): 9.66 (s, 1H, OH), 7.20-7.88 (m, 8H, Ar–H), 2.22 (s, 1H, NH), 1.87-2.08 (s, 2H, CH_2) and 0.84-0.97 (s, 3H, CH_3); ^{13}C NMR (100 MHz, acetone-d_6, δ ppm): 166.0 (2C, CO), 123.0-150.0 (14C, Ar–C), 54 (1C, CS) and 35.0 (2C, CH). m.f.: $C_{19}H_{15}ClN_4O_4S$. MS (*m/z*): 430 (M^+).

***N*-(2-(2-Hydroxy-7-(2,2,2-trifluoroethyl)quinolin-3-yl)-4-oxothiazolidin-3-yl)isonicotinamide (SK-7):** Light greyish-white solid (yield: 76%; m.p.: 192-194 ºC; R_f value: 0.60); IR (KBr, ν_{max}, cm^{-1}): 3385 (NH), 3170 (OH), 3006 (CH), 1653 (C=O), 1507 (C=C), 1490 (C–C), 1170 (CS), 1120-1228 (CF), 1066 (CN); ^{1}H NMR (400 MHz, $CDCl_3$, δ ppm): 11.24 (s, 1H, NH), 9.25 (s, 1H, OH), 7.07-7.42 (m, 7H, Ar–H), 5.34 (s, 1H, CH), 3.70-4.13 (s, 2H, CH_2), 2.05-2.32 (s, 2H, CH_2); ^{13}C NMR (100 MHz, acetone-d_6, δ ppm): 166.0 (2C, CO), 125.0-150.0 (14C, ArC), 117 (1C, CH), 37 (1C, CS). m.f.: $C_{20}H_{15}F_3N_4O_3S$. MS (*m/z*): 448 (M^+).

***N*-(2-(2-Hydroxy-7-(4-hydroxy-2-nitrophenyl)quinolin-3-yl)-4-oxothiazolidin-3-yl)isonicotinamide (SK8):** Light white solid (yield: 73%; m.p.: 194-196 ºC; R_f value: 0.60); IR (KBr, ν_{max}, cm^{-1}): 3537 (NH), 3335 (OH), 2953 (CH), 1658 (C=O), 1576 (C=C), 1170 (CS); ^{1}H NMR (400 MHz, $CDCl_3$, δ ppm): 11.23 (s, 1H, NH), 9.56-9.68 (s, 2H, OH), 7.47-8.18 (m, 11H, Ar–H), 5.40 (s, 1H, CH) and 3.60-3.66 (s, 1H, CH); ^{13}C NMR (100 MHz, acetone-d_6, δ ppm): 166.0 (2C, CO), 125.0-148.0 (20C, Ar–C), 57.0 (1C, CH) and 37 (1C, CS). m.f.: $C_{24}H_{17}N_5O_6S$. MS (*m/z*): 503 (M^+).

N-(2-(7-(2-Cyano-4-hydroxyphenyl)-2-hydroxyquinolin-3-yl)-4-oxothiazolidin-3-yl)isonicotinamide (SK-9): Light white solid (yield: 76%; m.p.: 201-203 ºC; R_f = 0.7); IR (KBr, ν_{max}, cm^{-1}): 3408 (NH), 3125 (OH), 3034 (CH), 2111 (C≡N), 1684 (C=O), 1628, 1507 (C=C), 1153 (C–S), 1049 (N–N), 870 (CN); ^{1}H NMR (400 MHz, DMSO-d_6, δ ppm): 10.97 (s, 1H, NH), 9.89 (s, 2H, OH), 7.20-7.37 (m, 11H, Ar–H), 5.08 (s, 1H, CH), 3.65-3.93 (s, 1H, CH_2), 2.48 (s, 1H, DMSO); ^{13}C NMR (100 MHz, acetone-d_6, δ ppm): 166 (2C, C=O), 123-147 (20C, Ar–C), 115 (1C, C≡N), 56 (1C, CH), 35 (1C, CH_2). m.f.: $C_{25}H_{17}N_5O_4S$. MS (*m/z*): 383 (M^+).

***N*-(2-(7-(2-Bromo-4-hydroxyphenyl)-2-hydroxyquinolin-3-yl)-4-oxothiazolidin-3-yl)isonicotinamide (SK-10):** Off-white solid (yield: 72%; m.p.: 187-189 ºC; R_f = 0.72); IR (KBr, ν_{max}, cm^{-1}): 3123 (NH), 3056 (OH), 2924 (CH), 1684 (CO), 1526 (C=C), 1474 (C–C), 1163 (CS), 669 (-Br); ^{1}H NMR (400 MHz, $CDCl_3$, δ ppm): 11.72 (s, 1H, NH), 10.11 (s, 1H, OH), 7.10-7.95 (m, 11H, Ar–CH), 5.50 (s, 1H, CH), 3.55 (s, 1H, CH). ^{13}C NMR (100 MHz, acetone-d_6, δ ppm): 166.0 (1C, C=O), 122-140 (20C, Ar–C), 52 (1C, CH), 35.0 (1C, CS). m.f.: $C_{24}H_{17}BrN_4O_4S$. MS (*m/z*): 536 (M^+).

2-Amino-6-fluoro-*N*-(2-(2-hydroxyquinolin-3-yl)-4-oxothiazolidin-3-yl)-3-(2-methylcyclopropyl)-5-(trifluoromethyl)isonicotinamide (SK-11): Pale greenish-yellow solid (yield: 63%; m.p.: 192-194 ºC; R_f = 0.82); IR (KBr, ν_{max}, cm^{-1}): 3293 (OH), 2942 (CH), 1668 (C=O), 1586 (C=C), 1457 (C–C), 1151 (CS), 683 (CF); ^{1}H NMR (400 MHz, $CDCl_3$, δ ppm): 11.75 (s, 1H, NH), 9.37 (s, 1H, OH), 7.27-7.83 (m, 5H, Ar–H), 4.93 (s, 1H, CH), 3.74 (s, 1H, CH), 2.14 (s, 1H, CH), 1.26-1.29 (s, 2H, CH_2), 0.88 (s, 3H, CH_3); ^{13}C NMR (100 MHz, acetone-d_6, δ ppm): 166-171 (2C, C=O), 124-146 (14C, Ar–C), 52 (1C, CH), 32 (1C, CH), 25 (1C, C), 24 (1C, CH), 11-20 (3C, CH). m.f.: $C_{23}H_{19}F_4N_5O_3S$. MS (*m/z*): 521 (M^+).

2-Ethynyl-5-(2-fluorocyclopropyl)-*N*-(2-(2-hydroxyquinolin-3-yl)-4-oxothiazolidin-3-yl)-6-methyl-3-(trifluoromethyl)isonicotinamide (SK-12): Light cream solid (yield: 73%; m.p.: 172-174 ºC; R_f = 0.62). IR (KBr, ν_{max}, cm^{-1}): 3554 (NH), 3127 (OH), 2968 (CH), 1638 (C=O), 1576 (C=C), 1466 (C–C), 1172 (CS), 1013-1084 (CF), 719 (C≡C); ^{1}H NMR (DMSO-d_6, δ ppm): 10.19 (s, 1H, NH), 9.25 (s, 1H, OH), 7.36-7.53 (m, 5H, Ar–H), 5.07 (s, 1H, CH), 5.02 (s, 2H, NH_2), 6.85 (s, 1H, C–C), 4.08 (s, 1H, CH), 3.69 (s, 3H, CH_3), 1.39 (s, 2H, CH_2); ^{13}C NMR (100 MHz, acetone-d_6, δ ppm): 162 (2C, C=O), 121–143 (14C, Ar–C), 121 (1C, C–F_3), 51 (1C, CH), 32 (1C, C≡C), 15 (2C, CH_2). m.f.: $C_{25}H_{18}F_4N_4O_3S$. MS (*m/z*): 530 (M^+).

Biological assays

Microplate Alamar blue assay (MABA): *In vitro* antimycobacterial activity of the synthesized hybrid compounds was confirmed against non-replicating and replicating MTB through Microplate Alamar Blue Assay (MABA) and Low Oxygen Recovery Assay (LORA) methods [19]. The concentration of tested substances varied from 100 to 0.39 µg/mL. There was a sterile control and a growth control made on separate plates, one without antitubercular and the other without inoculation. The controls and plates were kept at 37 ºC for 7 days [20]. After the incubation time was up, an Alamar blue solution was added to each plate well. The plates were then incubated again for 24 h. Growth is shown by colour shift from blue to pink and the lowest concentration of chemical that inhibited the colour change was documented as its MIC. In this work, isoniazid was used as standard drug.

Computational studies

Molecular docking studies: Molecular docking studies were performed to evaluate binding interactions of synthesized compounds with *M. tuberculosis* Enoyl-ACP reductase (InhA) enzyme. The crystal structure of InhA (PDB ID, *e.g.*, 5JFO) was retrieved from RCSB Protein Data Bank. The enzyme's three-dimensional crystal structure was sourced from RCSB Protein Data Bank and processed to remove all crystallographic water molecules and co-crystallized ligands. This was followed by addition of polar hydrogens and Kollman charges using AutoDock Tools (v1.5.7). Ligand structures. Docking simulations were executed with AutoDock Vina, active site around coordinates of crystallized ligand. The grid box was centred at include entire catalytic site.

QSAR model: A quantitative structure-activity relationship (QSAR) model was developed to correlate chemical structures of **SK-1–SK-12** compounds with their antitubercular activity (MIC values from MABA). Molecular were calculated for each compound using the PaDEL-Descriptor software (v2.21). The 2D structures were first optimized using MMFF94 force field. A large was generated from which a relevant subset was selected based on variance inflation factor (VIF) analysis and correlation with the biological activity. Multiple linear regression was used to build QSAR model. The quality of the model was evaluated using correlation coefficient (R^2) and cross-validation parameters (Q^2).

RESULTS AND DISCUSSION

Novel quinoline–thiazolidinone–isonicotinamide hybrids (**SK-1 to SK-12**) were synthesized starting from substituted 2-chloroquinoline-3-carbaldehydes (**1a-l**), obtained *via* Vilsmeier-Haack formylation of substituted N-phenylacetamides using DMF/$POCl_3$, followed by alkaline hydroysis to obtain the corresponding 2-hydroxyquinoline-3-carbaldehydes (**2a-l**). Subsequent condensation with isoniazid (INH) in DMSO/EtOH afforded the Schiff bases (**3a-l**), which were then cyclized with thioglycolic acid to give the final thiazolidinone derivatives (**SK-1** to **SK-12**). All the synthesized compounds showed the characteristic IR absorptions for OH/NH, C=O, C=N/C=C, and C–S, and their $^1H/^{13}C$ NMR spectra confirmed quinolinyl, thiazolidinone, and isonicotinamide moieties. The MS (M^+ peaks) also matched the expected molecular formulas, supporting successful synthesis and structural integrity.

Antitubercular activity: The antitubercular activity was evaluated against *M. tuberculosis* H37Rv (ATCC 27294) and three clinical multidrug-resistant (MDR) strains using the microplate Alamar Blue assay (MABA) and the low-oxygen recovery assay (LORA). The minimum inhibitory concentrations (MIC) were determined in triplicate and the results are presented in Table-1. Several derivatives **SK-5**, **SK-3** and **SK-6** showed significant anti-tubercular activity in MABA and LORA method with MIC (13.5 µg/mL and 18.25 µg/mL. In the LORA technique likewise, the identical compound **SK-5** displayed substantial activity with MIC 08.25 and 14.53 µg/mL. Hence, aliphatic group substitution at quinoline nucleus enhances the anti-tubercular action than aromatic substituted drugs. Among the aromatic substituted triazole analogues, compound **SK-3** demonstrated considerable anti-tubercular activity with MIC 10.52 and 2.03 µg/mL, in MABA and LORA techniques, respectively. From these acquired activity spectra, it has been concluded that drugs having electron-donating groups promote anti-TB action. In contrast, compounds containing electron withdrawing substitution lowers the total anti-TB action.

TABLE-1
MINIMUM INHIBITORY CONCENTRATION (MIC) OF SYNTHESIZED COMPOUNDS AGAINST *M. tuberculosis*

Compounds	MABA MIC (µg/mL)	LORA MIC (µg/mL)
SK-1	42.23	42.84
SK-2	33.25	32.35
SK-3	10.52	12.03
SK-4	38.25	36.87
SK-5	08.25	14.53
SK-6	13.50	18.25
SK-7	40.93	41.60
SK-8	45.22	48.86
SK-9	41.43	44.75
SK-10	50.06	41.69
SK-11	52.34	48.05
SK-12	42.29	47.51
Isoniazid	0.39	2.56

Molecular docking and QSAR analysis: The synthesized hybrid compounds exhibited varying binding affinities toward the target protein (Table-2). Among them, compound **SK-5** demonstrated the strongest binding affinity of -9.3 kcal/mol, forming hydrogen bonds with GLU56, LEU83, ASP54, SER20, GLU92, MET147, ILE194, PHE149 and TYR192. Fig. 1 illustrates the binding affinities and interaction profiles of the synthesized compounds with the target protein. Compound **SK-3** also exhibited a high affinity of -9.1 kcal/mol, indicating increased stability through aromatic and hydrophobic interactions. Compound **SK-8** showed a binding energy of -8.1 kcal/mol, with interactions primarily hydrophobic and involving π–π stacking with ARG144, PHE149, ILE194 and MET147. Compound **SK-11** displayed a binding energy of -7.8 kcal/mol, interacting with TYR196, PHE149, GLU192, ILE194, SER94, and PHE143 through carbon–hydrogen bonds, alkyl and π–alkyl hydrophobic packing and aromatic interactions.

TABLE-2
MOLECULAR DOCKING RESULTS FOR SYNTHESIZED COMPOUNDS (**SK-1** to **SK-12**) AND ISONIAZID

Compound	Affinity (Kcal/mol)	Amino acid residues
SK-1	-8.1	ARG144, PHE149, ILE194, MET147
SK-2	-8.9	MET147, SER20, ASP54, TYR192, GLY148, MET147
SK-3	-9.1	THR88, ARG144, GLY148, PHE149
SK-4	-8.7	GLY148, PHE149, TYR192, ILE194, MET147
SK-5	-9.3	GLU56, LEU83, ASP54, SER20, GLU92, MET147, ILE194, PHE149, TYR192
SK-6	-9.1	TYR A:196, PHE A:149, GLU A:192, ILE A:194, SER A:94, PHE A:143
SK-7	-8.3	THR88, ASP54, TYR192, PHE149
SK-8	-8.6	GLU92, ASP54, LEU83, PHE149, VAL167
SK-9	-8.0	SER20, GLU92, TYR192, PHE149
SK-10	-7.8	ASP54, GLU92, MET147, PHE149, TYR192
SK-11	-8.5	SER20, ASP54, GLU92, MET147, PHE149
SK-12	-7.5	ALA A:191, MET A:147, PHE A:148, GLU A:256, LEU A:83
Isoniazid	-7.5	GLN 66, PHE-41, GLY-96, ASP-64

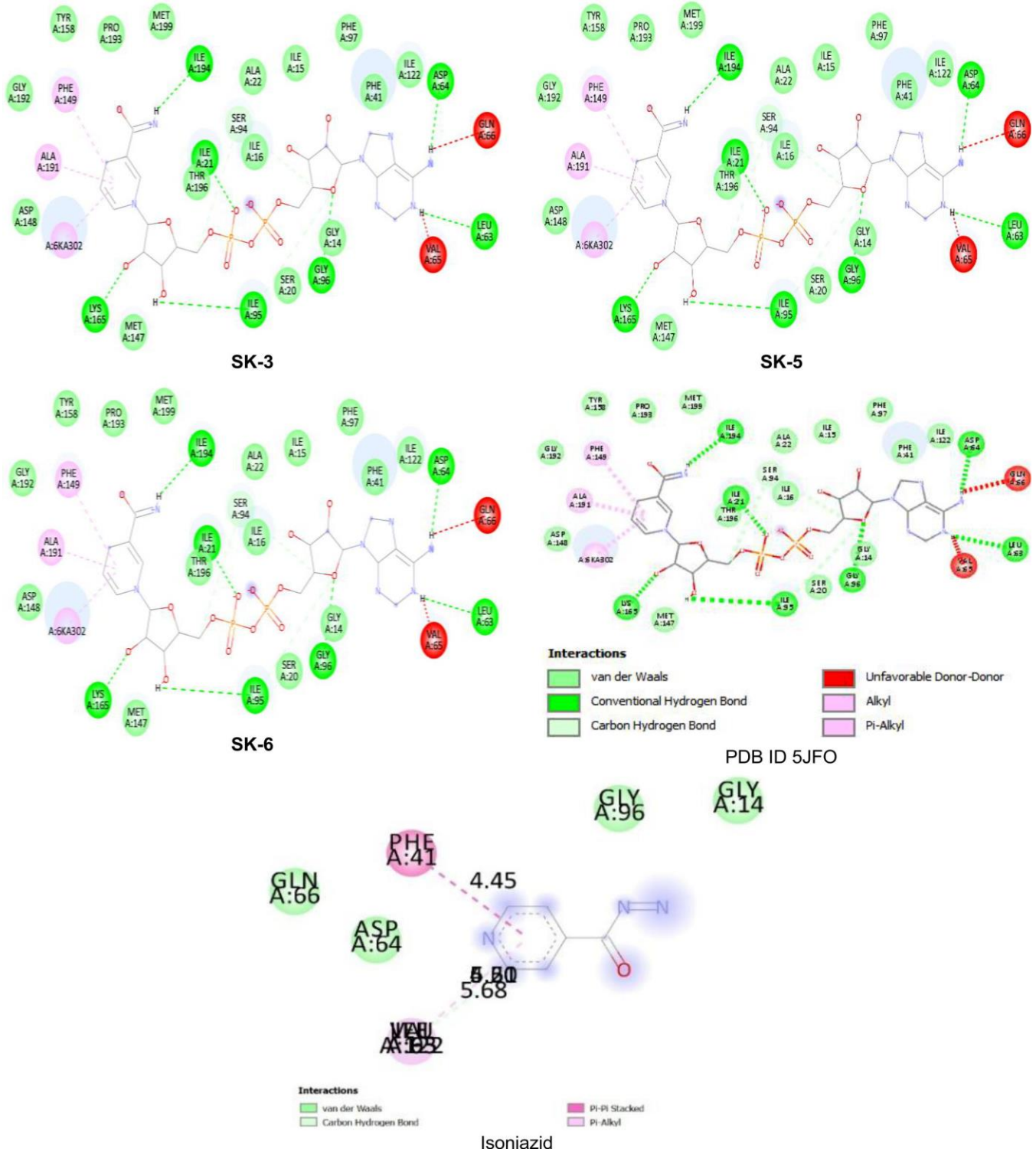

Fig. 1. 2D Representation of the binding modes of novel triazole-linked compounds and isoniazid to DNA gyrase and enoyl-[acyl-carrier-protein] reductase (**SK-3**, **SK-5** and **SK-6** with isoniazid)

Compound **SK-2** demonstrated the stable polar and hydrophobic contacts with SER20, ASP54, TYR192, GLY148, and MET147, with an affinity of -8.9 kcal/mol, whereas compound **SK-4** bound at -8.7 kcal/mol through hydrogen bonds and π-alkyl interactions with GLU92, ASP54, LEU83, PHE149, and VAL167. Compound **SK-8** showed an affinity of -8.6 kcal/mol, stabilized by π-alkyl and alkyl interactions with GLY148, PHE149, TYR192, ILE194 and MET147, whereas compound **SK-11** interacted with SER20, ASP54, GLU92, MET147 and PHE149 at -8.5 kcal/mol, favouring polar contacts within the catalytic site.

Compound **SK-7** exhibited π-alkyl interactions with THR88, ASP54, TYR192 and PHE149, corresponding to -8.3 kcal/mol whereas compound **SK-9** achieved -8.0 kcal/mol

through π-alkyl interactions with SER20, GLU92, TYR192, and PHE149, complemented by hydrogen bonds and van der Waals contacts with ASP54, GLU92, MET147, PHE149, and TYR192. Compound **SK-12** displayed a less favourable binding energy of -7.5 kcal/mol, interacting with ALA191, MET147, PHE148, GLU256, and LEU83.

ADMET prediction: The ADMET properties of synthesized compounds (**SK-1** to **SK-12**) was predicted using Swiss-ADME and pkCSM. All compounds adhered to Lipinski's rule of five without violations, indicating favourable oral bioavailability (Table-3). However, molecule 2 had one violation of the Veber rule due to an elevated topological polar surface area (TPSA > 140 Å^2). The molecular weight (MW) of all compounds was below optimal threshold of 500 Da, good membrane permeability. The consensus logP values varied from about 1.8 to 3.5 a balanced profile of hydrophilic and lipophilic properties that support oral absorption. Most compounds were predicted to have high gastrointestinal (GI) absorption. Molecule 2 was only exception, predicted to have low GI absorption due to its higher polarity and increased hydrogen bonding capacity (HBA = 7, HBD = 4). None of compounds were blood-brain barrier (BBB) which could help reduce side effects related to central nervous system. However, all compounds were substrates for P-glycoprotein (P-gp), which may affect efflux related resistance compounds are distributed in body. The inhibition profiles for cytochrome P450 (CYP) showed that several compounds might inhibit CYP1A2, with some also inhibiting CYP3A4 or CYP2C9 isoforms. The bioavailability score was consistently predicted at 0.55, indicating moderate oral bioavailability. Synthetic accessibility scores ranged from 3.6 to 4.1. All molecules are moderately complex and can be synthesized without too much difficulty. Overall, the ADMET predictions indicate that most compounds have favourable physico-chemical and pharmacokinetic properties that make them suitable for further lead development, with molecules 1, 3, 4 and 5 showing the most balanced profiles.

Physico-chemical profiles: Table-4 shows that all the synthesized compounds possessed molecular weights ranging from 366.39 to 537.39 Da, which generally fall within the acceptable range for drug-like molecules (< 500 Da). However, **SK-10**, **SK-11** and **SK-12** slightly exceeded this threshold, which may negatively influence membrane permeability. The topological polar surface area (TPSA) values varied between 120.72 and 186.77 Å^2. Compounds **SK-2**, **SK-8** and **SK-9** exhibited TPSA values above 140 Å^2, which could contribute to reduced membrane permeability and lower oral absorption. Hydrogen bond donor (HBD ≤ 5) and acceptor (HBA ≤ 10) counts were within the standard limits across the series, indicating generally acceptable hydrogen-bonding characteristics for oral bioavailability.

TABLE-3
ADME AND DRUG-LIKENESS PREDICTION FOR SYNTHESIZED COMPOUNDS (**SK-1** to **SK-12**)

Compound	GI absorption	BBB permeant	Pgp substrate	CYP1A2 inhibitor	CYP2C19 inhibitor	CYP2C9 inhibitor	CYP2D6 inhibitor	CYP3A4 inhibitor	log Kp (cm/s)
SK-1	High	No	Yes	Yes	No	No	No	No	-7.01
SK-2	Low	No	Yes	No	No	No	No	No	-7.71
SK-3	High	No	Yes	Yes	No	Yes	No	Yes	-6.84
SK-4	High	No	Yes	Yes	No	Yes	Yes	Yes	-6.62
SK-5	High	No	No	Yes	Yes	Yes	Yes	Yes	-6.02
SK-6	High	No	Yes	Yes	Yes	Yes	Yes	Yes	-7.10
SK-7	High	No	No	No	Yes	Yes	Yes	Yes	-6.54
SK-8	Low	No	No	No	Yes	Yes	No	Yes	-7.06
SK-9	Low	No	No	No	Yes	Yes	No	Yes	-7.02
SK-10	Low	No	No	No	Yes	Yes	No	Yes	-6.66
SK-11	Low	No	Yes	No	No	No	No	No	-6.44
SK-12	Low	No	Yes	No	No	Yes	Yes	Yes	-6.48

TABLE-4
PHYSICO-CHEMICAL PROPERTIES AND MOLECULAR DESCRIPTORS OF SYNTHESIZED COMPOUNDS (**SK-1** to **SK-12**)

Molecule	M.W	Log P	HBD	MR	TPSA	HBA	Bioavailability score	Synthetic accessibility
SK-1	430.86	-7.10	2	112.0	130.0	6	0.55	3.80
SK-2	448.42	-6.54	2	111.1	120.7	8	0.55	3.83
SK-3	503.49	-7.06	3	137.4	186.8	8	0.17	4.28
SK-4	483.50	-7.02	3	133.3	164.7	7	0.55	4.15
SK-5	537.39	-6.66	3	136.3	141.0	6	0.55	4.17
SK-6	396.42	-7.21	2	107.6	130.0	6	0.55	3.79
SK-7	472.52	-6.53	2	133.1	130.0	6	0.55	4.16
SK-8	521.49	-6.44	3	127.8	146.7	9	0.55	4.85
SK-9	528.51	-7.21	3	132.5	156.5	9	0.55	4.86
SK-10	530.49	-6.48	2	131.6	120.7	9	0.55	4.95
SK-11	554.94	-5.84	2	133.5	120.7	9	0.55	4.88
SK-12	611.05	-5.79	2	152.6	120.7	9	0.17	5.39

Drug-likeness rules: Fig. 2 shows that all compounds complied with Lipinski's rule of five, except **SK-8**, which exhibited two violations due to its molecular weight and topological polar surface area (TPSA). Compounds **SK-3**, **SK-5** and **SK-6** also showed deviations.

Metabolism (CYP inhibition): Various compounds were computationally predicted to inhibit CYP1A2, CYP2C9 and CYP3A4 (*e.g.* **SK-3 to SK-7**) indicating drug–drug interaction potential. Compounds **SK-8 to SK-12** had broader CYP inhibition profiles, potentially making pharmacokinetic behaviour complicated and necessitating additional *in vitro* metabolic stability studies.

Synthetic accessibility: Table-5 reparented as synthetic accessibility scores varied between 3.67 (**SK-1**) and 4.95 (**SK-12**), indicating moderate synthetic complexity. The latter values (**SK-8 to SK-12**) indicate higher structural complexity diversity of functional groups.

***In silico* pharmacological toxicity profiling of hybrid derivatives:** The synthesized hybrids **SK-1** through **SK-12** and additional analogs a consistent profile across various endpoints in pharmacological toxicity studies using ProTox-3.0 predictions [21]. Fig. 3 shows an Organ toxicities were predominantly active for hepatotoxicity (probabilities ranging from 0.51 to 0.69) neurotoxicity (0.57 to 0.87), nephrontoxicity (0.50 to 0.90), respiratory toxicity (0.67 to 0.98) and clinical toxicity (0.53 to 0.67) while cardiotoxicity inactive (0.72 to 0.82). As 7 blood-brain barrier permeability was active (0.50 to 1.00) potentially neurotoxic effects. Toxicity endpoints showed that carcinogenicity (0.51-0.64), immunotoxicity (0.56-0.99), mutagenicity (0.52-0.97), cytotoxicity (0.56-0.93), ecotoxicity (0.53-0.73) and nutritional toxicity (0.58-0.74) were all inactive. This means that the hazards to the environment and to DNA are minimal. All of the Tox21 nuclear receptor signalling pathways were inactive. These pathways include aryl hydrocarbon receptor (0.71-0.97) androgen receptor (0.94-0.99) estrogen receptors (0.81-1.00) peroxisome proliferator-activated receptor gamma (0.70-0.99). The stress response pathways such as Nrf2 (0.88-0.94) heat shock factor (0.88-0.94) mitochondrial membrane potential (0.50-0.78), p53 (0.83-0.96) ATAD5 (0.82-0.99). Molecular thyroid hormone receptors (0.59-0.90), transthyretin (0.63-0.97), ryanodine receptor (0.58-0.98), GABA and glutamate receptors (0.61-0.99), acetylcholinesterase (0.69-0.89), constitutive androstane receptor (0.98-0.99), pregnane X receptor (0.54-0.92), NADH-quinone oxidoreductase (0.92-0.99), voltage-gated sodium channel (0.58-0.95), and Na^+/I^- symporter (0.79-0.98) also showed inactivity, suggesting minimal disruption to these pathways.

The *in silico* analysis highlights the novelty of this study through extensive molecular docking, with binding affinities ranging from -9.3 to -7.8 kcal/mol, surpassing isoniazid (-7.5 kcal/mol) against hypothetical targets such as InhA. Key interactions, including hydrogen bonds with ASP54 and PHE149, provide insight into structure–activity relationships (SAR) for compound optimization. ADMET profiling using SwissADME and pkCSM indicates favorable drug-likeness, with Lipinski compliance for all compounds except one, bioavail-

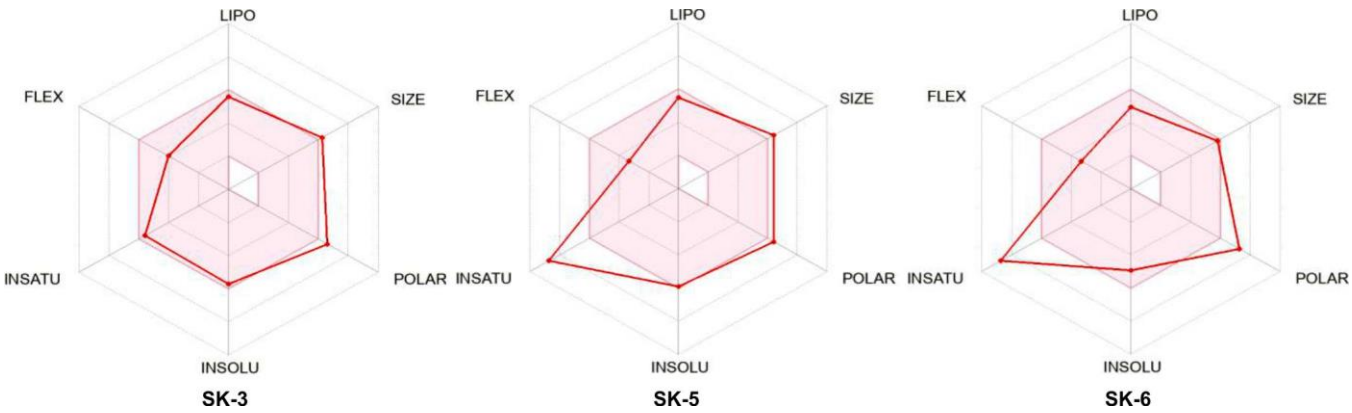

Fig. 2. *In silico* drug-likeness profile of analogues **SK-3**, **SK-5** and **SK-6**

TABLE-5
TOXICITY AND CYP450 INHIBITION PROFILE OF TEST COMPOUNDS

Compound	Hepatotoxicity	Neurotoxicity	Nephrotoxicity	Respiratory toxicity	CYP2C9 inhibition
SK-1	Active	Active	Inactive	Active	Inactive
SK-2	Active	Inactive	Active	Active	Inactive
SK-3	Active	Active	Active	Active	Inactive
SK-4	Active	Inactive	Active	Inactive	Inactive
SK-5	Active	Active	Active	Active	Inactive
SK-6	Active	Active	Active	Active	Inactive
SK-7	Active	Active	Inactive	Inactive	Inactive
SK-8	Active	Inactive	Inactive	Active	Inactive
SK-9	Inactive	Inactive	Active	Inactive	Inactive
SK-10	Inactive	Active	Inactive	Inactive	Inactive
SK-11	Inactive	Inactive	Inactive	Active	Inactive
SK-12	Inactive	Active	Inactive	Inactive	Inactive

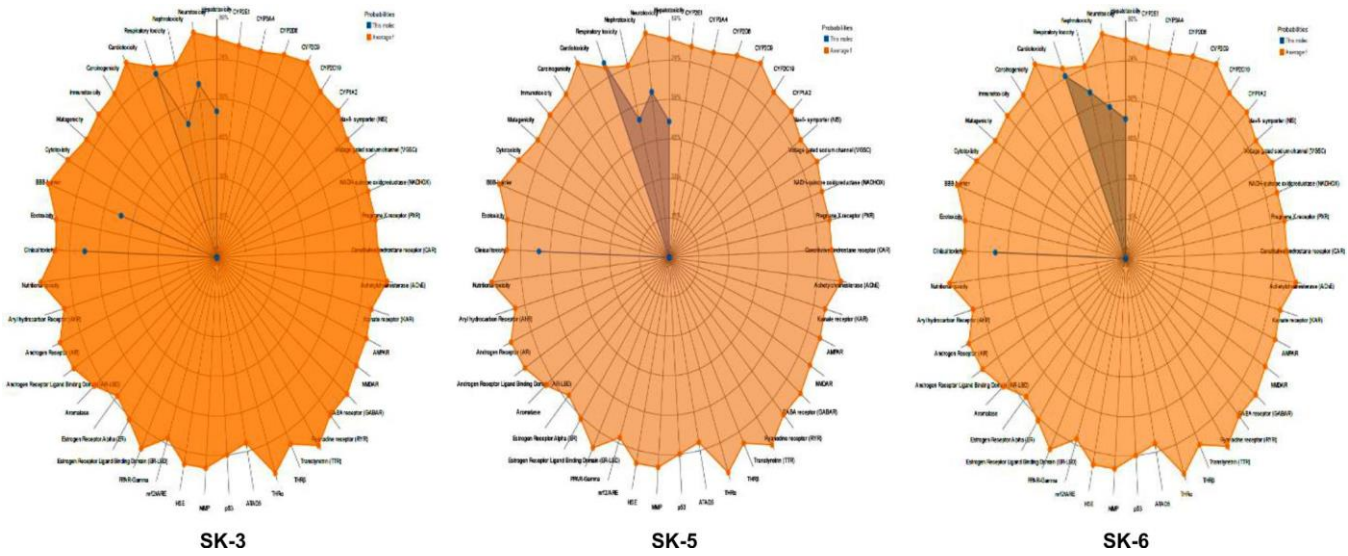

Fig. 3. Predicted toxicological profile of isoniazid *via* radar chart (**SK-3**, **SK-5** and **SK-6**)

ability scores of 0.55, moderate synthetic accessibility (3.6-4.95), high gastrointestinal absorption for many analogues, and low blood-brain barrier permeability to minimize CNS toxicity. Toxicity predictions from ProTox-3.0 suggest low risks for carcinogenicity, mutagenicity, and endocrine disruption, while potential organ-specific effects such as hepatotoxicity can guide safer lead selection.

Conclusion

Novel quinoline-thiazolidinone-isonicotinamide hybrids (**SK-1** to **SK-12**) were designed, synthesized, characterised and evaluated for their *in-vitro* antimycobacterial activity against non-replicating and replicating MTB through LORA and MABA techniques. The derivatives **SK-3**, **SK-5** and **SK-6** was found to be more potent with MIC value in MABA and LORA methods with **SK-3** (10.52 and 12.03), **SK-5** (08.25 and 14.53) and **SK-6** (13.5 and 18.25). These derivatives have promising ADMET profiles (*e.g.* Lipinski compliance moderate logP 0.93-4.31, high GI absorption for the majority), making them good leads for potential antitubercular agents.

CONFLICT OF INTEREST

The authors declare that there is no conflict of interests regarding the publication of this article.

REFERENCES

1. K.M. Dousa, S.G. Kurz, C.M. Bark, R.A. Bonomo and J.J. Furin, Infect. Dis. Clin. North Am., 34, 863 (2020); https://doi.org/10.1016/j.idc.2020.06.001
2. R.M.D. de Almeida, Internship and Monograph Teports Multidrug-resistant Tuberculosis: A Public Health Emergency, Epidemiological Analysis and New Therapeutic Approaches (2021); https://estudogeral.uc.pt/handle/10316/92970 (accessed on August 11, 2025).
3. H. Lv, X. Zhang, X. Zhang, J. Bai, S. You, X. Li, S. Li, Y. Wang, W. Zhang and Y. Xu, *BMC Infect. Dis.*, **24**, 243 (2024); https://doi.org/10.1186/s12879-024-09079-5
4. S. Dhingra, N.A.A. Rahman, E. Peile, M. Rahman, M. Sartelli, M.A. Hassali, T. Islam, S. Islam and M. Haque, *Front. Public Health*, **8**, 535668 (2020); https://doi.org/10.3389/fpubh.2020.535668
5. S. Rajendran, K. Sivalingam, R.P. Karnam Jayarampillai, W.L. Wang and C.O. Salas, *Chem. Biol. Drug Des.*, **100**, 1042 (2022); https://doi.org/10.1111/cbdd.14044
6. R. Patil, J. Chavan, S. Patel and A. Beldar, *Turk. J. Chem.*, **45**, 1299 (2021); https://doi.org/10.3906/kim-2106-5
7. K. Kumar, S. Puri and V. Abbot, *J. Heterocycl. Chem.*, **62**, 944 (2025); https://doi.org/10.1002/jhet.70048
8. W. Drzał and N. Trotsko, *Molecules*, **30**, 2201 (2025); https://doi.org/10.3390/molecules30102201
9. L.M. Ferreira, P. García-García, P.A. García and M.Á. Castro, *Eur. J. Pharm. Sci.*, **209**, 107097 (2025); https://doi.org/10.1016/j.ejps.2025.107097
10. V. Yadav, J. Reang, V. Sharma, J. Majeed, P.C. Sharma, K. Sharma, N. Giri, A. Kumar and R.K. Tonk, *Chem. Biol. Drug Des.*, **100**, 389 (2022); https://doi.org/10.1111/cbdd.14099
11. D. Tiglani, S. Salahuddin, A. Mazumder, R. Kumar and S. Mishra, *Int. J. Pharm. Res.*, **13**, 4605 (2021); https://doi.org/10.31838/ijpr/2021.13.01.582
12. Y.V.D. Nageswar, K. Ramesh and K. Rakhi, *Curr. Green Chem.*, **12**, 234 (2025); https://doi.org/10.2174/0122133461335061241101114827
13. S. Nirwan, V. Chahal and R. Kakkar, *J. Heterocycl. Chem.*, **56**, 1239 (2019); https://doi.org/10.1002/jhet.3514
14. S.K. Bera, M. Irfan and A. Porcheddu, *ChemCatChem*, **17**, e202401813 (2025); https://doi.org/10.1002/cctc.202401813
15. M.S. Tople, N.B. Patel and P.P. Patel, *J. Iran. Chem. Soc.*, **20**, 1 (2023); https://doi.org/10.1007/s13738-022-02648-y
16. L. Mohammadkhani and M.M. Heravi, *Front. Chem.*, **8**, 580086 (2020); https://doi.org/10.3389/fchem.2020.580086
17. S.G. Alegaon, V. U, K.R. Alagawadi, D. Kumar, R.S. Kavalapure, S.D. Ranade, S. Priya A and S.S. Jalalpure, *J. Biomol. Struct. Dyn.*, **40**, 6211 (2022); https://doi.org/10.1080/07391102.2021.1880479
18. P. Seboletswe, N. Cele and P. Singh, *ChemMedChem*, **18**, e202200618 (2023); https://doi.org/10.1002/cmdc.202200618
19. A. Nandikolla, S. Srinivasarao, Y.M. Khetmalis, B.K. Kumar, S. Murugesan, G. Shetye, R. Ma, S.G. Franzblau and K.V.G.C. Sekhar, *Toxicol. in Vitro*, **74**, 105137 (2021); https://doi.org/10.1016/j.tiv.2021.105137
20. D. Panigrahi and S.K. Sahu, *ACS Omega*, **10**, 46964 (2025); https://doi.org/10.1021/acsomega.5c05103
21. N. Saini, A. Sharma, V.K. Thakur, C. Makatsoris, A. Dandia, M. Bhagat, R.K. Tonk and P.C. Sharma, *Curr. Res. Green Sustain. Chem.*, **3**, 100021 (2020); https://doi.org/10.1016/j.crgsc.2020.100021